cation radical due to macrocycle reduction allows the π-radical orbital to interact with the iron d orbital, resulting in antiferromagnetic coupling. In this case, the magnetic coupling constant is expected to be small, because the a_2 radical orbital does not have large spin densities at pyrrole nitrogens.[13,24,25] Suppose that the triplet state of the (OEiBC)$Fe^{II}NO$ π-cation radical possesses slightly higher energy than the singlet state due to moderate spin coupling. The triplet state can be thermally admixed to the singlet state at room temperature. It is therefore likely that NMR hyperfine shifts are represented as a fractional weighted average of the limiting shifts of two extreme states. Then, a simulation of the Curie law plot for the (OEiBC)$Fe^{II}NO$ π-cation radical was performed by taking into account the magnetic interaction given by the Hamiltonian $\mathcal{H} = -J\mathbf{S}_1\cdot\mathbf{S}_2$, where $\mathbf{S}_1$ and $\mathbf{S}_2$ are spin vectors for the NO and π-radical spins.[39] As shown in Figure 6b, the coupling constant of $J = -46$ cm^{-1} fits well with the experimental values, and a content proportion of the triplet state at 296 K was estimated to be 35%. These results demonstrate that the NO and π-radical spins are weakly antiferromagnetically coupled and this thermal admixture is nearly saturated at room temperature.

Biological Implications. The sixth ligand of heme d_1 in a dissimilatory nitrite reductase has been shown to be nitrogenous ligand (probably the imidazole group of a histidyl residue) by ESR spectra of a NO-bound heme d_1, which has a superhyperfine structure due to an additional nitrogen atom.[6] On the other hand, the axial ligand for the siroheme in assimilatory nitrite reductases remains undetermined.[40] According to the results reported here, the axial ligation, if any, in assimilatory nitrite reductases may prefer the $Fe^{II}(NO^+)(L)$ complex (**5**) instead of the π-cation radical (**4**) as a reaction intermediate during the reduction of nitrite to nitric oxide, and **5** will readily release NO. As noted previously,[11] however, the subsequent reaction of nitric oxide to ammonia may require the $Fe^{II}NO$ π-cation radical (**4**) because of its stability.

In summary, (OEC)$Fe^{II}NO$ and (OEiBC)$Fe^{II}NO$ π-cation radicals were successfully prepared by chemical oxidation and their hyperfine-shifted NMR spectra have demonstrated that the radical orbitals for both π-cation radicals are of an a_2 type. Addition of imidazole to the π-radical solutions promoted valence isomerization to yield (OEC)$Fe^{II}(NO^+)$(Im) and (OEiBC)Fe^{II}-(NO^+)(Im). The model studies reported here certainly raised the possibility that the axial ligation may control the structures of the reaction intermediates and the reactivity of NO bound to iron in nitrite reductases.

To gain further insight into the magnetic interaction between the NO and π-radical spins, detailed studies of solid-state magnetic susceptibilities of the π-cation radicals are under investigation.

Acknowledgment. We thank Dr. T. Yoshimura for helpful discussions concerning syntheses of nitrosyl complexes and Dr. A. Yabe and Mr. T. Ohana for low-temperature IR measurements. We also thank Mr. Y. Ohta for some spectral measurements and Dr. Y. Watanabe and the reviewers for helpful comments.

(39) The simulation of the Curie law plot for (OEiBC)$Fe^{II}NO$ π-cation radical was performed with the following equation, $\delta_{obs} = [\delta'_{s=0}/T + 3(\delta'_{s=1}/T)\exp(-J/kT)]/(1 + 3\exp(-J/kT)) + \delta_{dia}$, where $\delta'_{s=0}/T$ and $\delta'_{s=1}/T$, with opposite signs, are the limiting shifts for the singlet and triplet states, respectively, J is an energy separation gap of the singlet and triplet states, and δ_{dia} is a diamagnetic correction based on the NMR shifts for the free base, H_2OEiBC.

(40) ESR spectra of spinach nitrite reductase–NO complexes have been observed.[7,8]

Enantioselective Binding of Tryptophan by α-Cyclodextrin

Kenny B. Lipkowitz,* Srinivasrao Raghothama, and Jia-an Yang

Contribution from the Department of Chemistry, Indiana University-Purdue University at Indianapolis, 1125 East 38th Street, Indianapolis, Indiana 46205. *Received July 1, 1991*

Abstract: ^{1}H and ^{13}C NMR studies of racemic and optically pure tryptophan binding with α-cyclodextrin are carried out to explain chiral recognition in this guest–host system. The changes in chemical shifts, coupling constants, and relaxation times for the *R* enantiomer are larger than for *S* upon binding, and differential changes of *R* vs *S* in the bound state are larger for the more tightly bound *R* enantiomer. An intermolecular NOE between guest and host places the indole ring near the secondary hydroxyl rim of the cyclodextrin for both enantiomers, suggesting similar modes of binding. Results extracted from molecular dynamics simulations are that both guests are highly localized on the interior of the host, the ammonium group of the zwitterionic tryptophan does not contribute to the recognition process, and the more tightly bound *R* enantiomer forms twice as many hydrogen bonds as its optical antipode, most of which are multiple-contact hydrogen bonds. Both *R* and *S* guests are found to use the same kinds of intermolecular interactions but to a greater or lesser extent. Armstrong's chiral recognition model has been slightly modified but generally remains intact.

Introduction

The intermolecular forces have been exhaustively studied and are thoroughly documented.[1] The way these forces act to form inclusion complexes is now the focus on ongoing studies in molecular recognition.[2] Less well understood but critical to many disciplines of science is chiral recognition. What are the origins of enantioselectivity? How does a chiral receptor, either natural or synthetic, discriminate between two nonsuperimposable mirror images that otherwise have identical molecular descriptors? Precisely how intermolecular forces act, in concert, to discriminate between enantiomers is not well established.

In this paper we examine the enantioselective binding of D,L-tryptophan to α-cyclodextrin (CD). We select tryptophan because it is size consistent with α-cyclodextrin and should form inclusion complexes[3] and it provides a starting point for future studies of how chiral recognition is enhanced or diminished by replacing the

(1) A well written introductory textbook exists: Rigby, M.; Smith, E. B.; Wakeham, W. A.; Maitland, G. C. *The Forces Between Molecules*; Oxford Science Publications, Clarendon Press: Oxford, 1986.

(2) (a) Cram, D. J. *Angew. Chem., Int. Ed. Engl.* **1988**, *27* (8), 1009. (b) Lehn, J.-M. *Ibid.* **1988**, *27* (8), 89. (c) Rebek, Jr., J. *Ibid.* **1990**, *29* (3), 245.

(3) (a) Bender, M. L.; Komiyama, M. *Cyclodextrin Chemistry*; Springer: New York, 1978. (b) Saenger, W. *Angew. Chem., Int. Ed. Engl.* **1980**, *19*, 344. (c) Szejtli, J. *Cyclodextrins and Their Inclusion Complexes*; Akademiai Kiado: Budapest, 1982. (d) Szejtli, J. *Cyclodextrin Technology*, Kluwer Academic Publishers: Dordrecht, 1988.

0002-7863/92/1514-1554$03.00/0

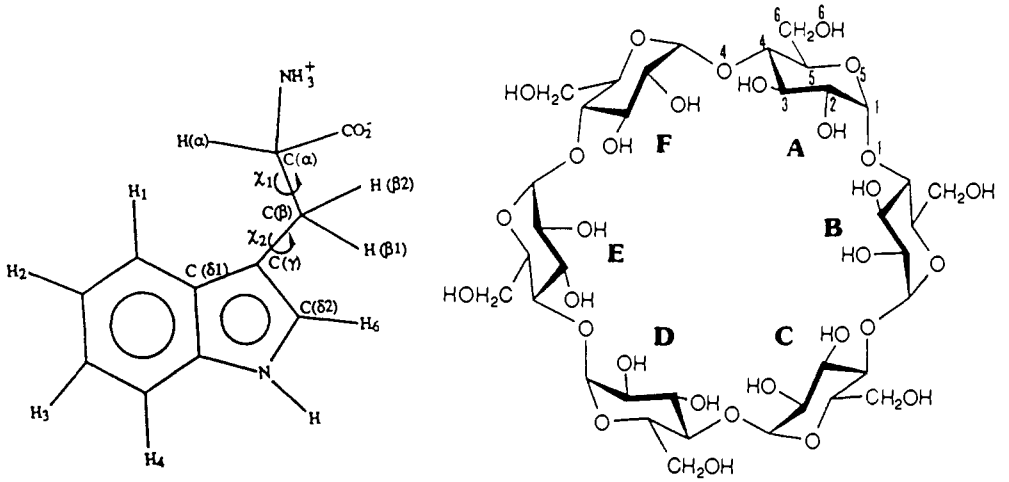

Figure 1. Atom-labeling scheme for tryptophan and α-cyclodextrin.

neutral zwitterion with positively or negatively charged groups.[4] We select α-CD as the chiral host because of the extensive literature background on CD complexation,[3] the recent flurry of activity to study and to use these macrocycles as microenvironments to induce asymmetric reactions,[5] and finally, in keeping with our research program,[6] it serves as the basic structure for chiral stationary phases used in gas, liquid, and supercritical fluid phase chromatographies.[7]

The specific questions we pose are the following: (1) What are the intermolecular forces responsible for substrate binding? (2) Where on or in the host does the substrate bind? (3) What are the differential interactions between host and guest that give rise to enantioselection? (4) What differences do (*R*)- and (*S*)-tryptophan experience in the chiral cavity? (5) Are existing chiral recognition mechanisms valid?

Experimental Section

All solvents and chemicals were obtained in spectroscopically pure form from Aldrich Chemicals and used as is. A stock solution of α-CD was prepared in 99.95% D_2O. The guest was added to this solution of α-CD which was then slightly warmed and sonicated for several hours. The guest to host ratio was maintained at 1:1 for the NMR studies. Solutions of 40 mM concentration were used unless specified otherwise.

All NMR experiments were performed on a General Electric QE-300 FT-NMR spectrometer operating at 300 MHz in the ^2H lock mode. The 75-MHz ^{13}C NMR spectra were recorded on the same spectrometer. Typical spectral width of 3600 Hz in 16K (20-bit) memory size was used. For a normal spectrum, 50–60° pulses with overall delay of 3 s between pulses were used. The time-domain data were exponentially multiplied before Fourier transformation with 0.0–0.5 Hz line broadening functions depending on the resulting S/N ratio of the spectrum. Tetramethylsilane (TMS) was used as internal reference for all spectra.

T_1 relaxation time measurements were made using the inversion recovery method. Seventeen different τ delays varying from 0.1 to 20 s between 180° and 90° pulses were used. The data obtained were fitted to the exponential equation $M = M_0(1 - 2e^{-\tau/T})$, where M_0 is the amplitude at $\tau \gg T$, M is the amplitude at τ, T is the delay time, and T is the fitted T_1 relaxation time.

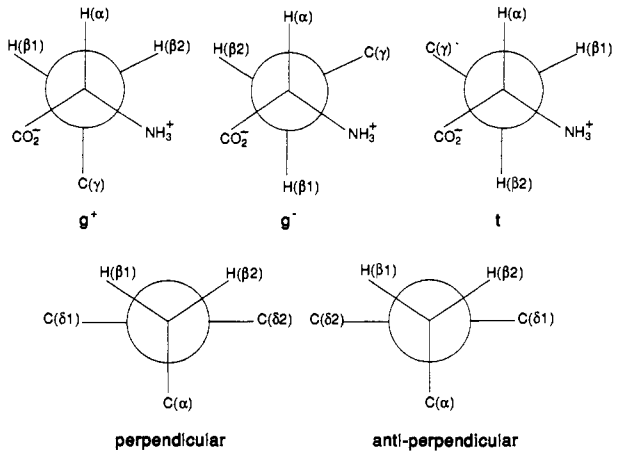

Figure 2. Possible rotameric states for tryptophan: top, gauche (+), gauche (−), and trans conformers corresponding to rotation about C_α–C_β; bottom, orthogonal orientations due to rotations about the C_α–C_β bond.

1-D difference NOE spectra were obtained by taking differences of two spectra. Low-power presaturation was done prior to pulse. While acquiring data, accumulation was switched alternately between scans, from on- to off-resonance irradiation, so that experimental errors cancel giving good difference spectra. Difference was taken after Fourier transforming the individual free induction decays using a larger line broadening function (on the order of 1 Hz). As the enhancements are around 5%, the difference spectra are blown up by a factor of 8 or 16 depending on the S/N ratio. Generally, several hundred accumulations were done for each irradiation.

Molecular modeling was done primarily with the CHARMM force field[8] as implemented in Polygen's QUANTA/CHARMM program.[9] Energy minimizations were carried out by steepest descent followed by adopted-basis Newton Raphson minimization. Dielectric of the medium was set at 1.5. Conformer searching of tryptophan involved grid searches. Beginning with a low-energy structure a double dihedral driver calculation was carried out in 10° increments. At each torsion angle the energy was minimized with 500 steepest descent minimizations. Minima on the resulting conformation potential energy surface were then fully optimized as above. The conformer search was done more than two times, beginning from different starting structures, to ensure the search was not sensitive to initial starting conditions.

Molecular dynamics simulations were carried out using Polygen's standard protocol with SHAKE.[10] Heating and equilibration time periods were followed by multiple production runs for data acquisition.

(4) Lipkowitz, K. B.; Green, K. Work in progress.

(5) Recent examples include: (a) Kawajiri, Y.; Motohashi, N. *J. Chem. Soc., Chem. Commun.* **1989**, 1336. (b) Komiyama, M.; Takeshige, Y., *J. Org. Chem.* **1989**, *54*, 4936. (c) Rao, V. P.; Turro, N. J. *Tetrahedron Lett.* **1989**, *30* (35), 4641. (d) Rao, K. R.; Sattur, P. B. *J. Chem. Soc., Chem. Commun.* **1989**, 342. (e) Sangwan, N. K.; Schneider, H.-J. *J. Chem. Soc., Perkin Trans. 2* **1989**, 1223. (f) Chung, W.-S.; Turro, N. J.; Silver, J.; leNoble, W. J. *J. Am. Chem. Soc.* **1990**, *112*, 1202.

(6) Lipkowitz, K. B.; Baker, B. *Anal. Chem.* **1990**, *62*, 770 and references therein.

(7) (a) Souter, R. W. *Chromatographic Separations of Stereoisomers*; CRC Press: Boca Raton, FL, 1985. (b) Allenmark, S. G. *Chromatographic Enantioseparation Methods and Applications*; Ellis Horwood: Chichester, 1988. (c) *Chiral Separations*; Stevenson, D., Wilson, I. D., Eds.; Plenum Press: New York, 1988. (d) Wainer, I. W. *A Practical Guide to the Selection and Use of HPLC Chiral Stationary Phases*; J. T. Baker: Phillipsburg, NJ, 1988. (e) *Chromatographic Chiral Separations*; Zief, M., Crane, L. J., Eds.; Marcel Dekker: New York, 1988. (f) *Chiral Liquid Chromatography*; Lough, W. J., Ed.; Blackie and Son: London, 1989.

(8) Brooks, B. R.; Bruccoleri, R. E.; Olafson, B. D.; States, D. J.; Swaminathan, S.; Karplus, M. *J. Comput. Chem.* **1983**, *4* (2), 187.

(9) QUANTA/CHARMM, Version 3.0. Polygen Corp., 200 Fifth Av., Waltham, MA 02254.

(10) Berendsen, H. J. C.; Postma, J. P. M.; DiNola, A.; Van Gunsteren, W. F.; Haak, J. R. *J. Chem. Phys.* **1984**, *81*, 3684.

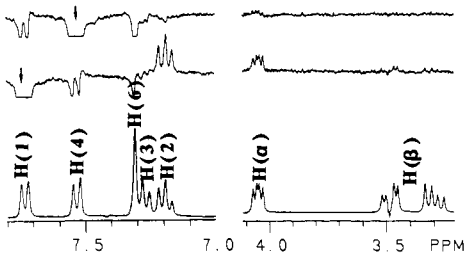

Figure 3. Bottom: ^{1}H NMR assignments for tryptophan. Top: NOE difference spectra on free tryptophan (the arrow indicates the peak irradiated).

Selection of initial binding sites and orientations of the guest within the host are explained in the text.

Results and Discussion

A. NMR Studies. 1. Free Guest and Host. Studies on conformational changes of tryptophan as a zwitterion have been reported both in solid and liquid states.[11] The tryptophan molecule and its atom labels are shown along with α-CD in Figure 1. χ_1 is the dihedral angle defined by NH_3–C_α–C_β–C_γ, and χ_2 is the dihedral angle defined by C_α–C_β–C_γ–C_δ. These torsion angles are the most important for defining the structural features of tryptophan. Figure 2 depicts the possible rotameric forms due to changes in χ_1 and χ_2. From crystal structures it was established that the tryptophan is almost invariably found in a perpendicular or antiperpendicular orientation;[11a,b] i.e., $\chi_2 = \pm 90°$. The most predominant structure is with $\chi_1 = -60°$ (g^-) and $\chi_2 = 90°$, but in solution, other conformers exist.[11d]

With this background we carried out NMR experiments on free tryptophan. Coupling constants J and chemical shifts δ are included along with other data that will soon be described (see Table III). To better understand the structural features of aqueous tryptophan, 1D-difference NOE experiments were done. The difference spectra are shown in Figure 3. The bottom trace shows the normal spectrum with proper assignments. In the top trace the H_4 aromatic doublet is irradiated. This would result in an NOE enhancement at the H_3 triplet which could not be properly seen because of irradiation power spillover. No other NOE was detected. The middle trace shows irradiation of the H_1 nucleus which results in not only NOE at its neighbor but also a substantial enhancement (~7%) on the H_α proton. For this to occur, the preferred conformation is the one where the two nuclei (H_1 and H_α) are in close proximity to one another (~3 Å). The magnitude of the H_1/H_α NOE, albeit large, need not reflect the prevalence for one conformation over another because, depending on the distance between H_1 and H_α, even a small population of one conformer can give rise to a strong observed NOE effect. Indeed, this aqueous conformation is inconsistent with the solid-state structure and does not conform with the lowest energy structure computed with the CHARMM force field, but rather is the next most stable conformer (vide infra) which has an H_1–H_α interatomic distance of 2.24 Å. These conformational changes of tryptophan in solution have been observed earlier.[11d,e]

The numbering scheme for the α-CD is shown in Figure 1. The 300-MHz ^{1}H NMR spectrum along with the 75-MHz proton coupled and decoupled ^{13}C NMR spectra are provided in the supplementary material as Figures S1 and S2. The chemical shifts and coupling constants are provided in supplementary Tables 1 and 2, respectively. The spectra and data in these tables agree well with existing literature values.[3,12] The NMR spectra are simple and provide sharp peaks representing a 6-fold axis of symmetry.

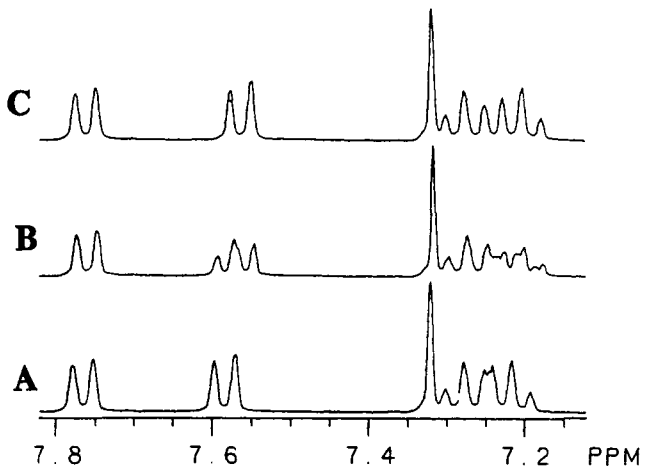

Figure 4. ^{1}H NMR spectra in the aromatic region of bound tryptophan: (A) (*R*)-tryptophan + α-cyclodextrin; (B) (*RS*)-tryptophan + α-cyclodextrin; (C) (*S*)-tryptophan + α-cyclodextrin.

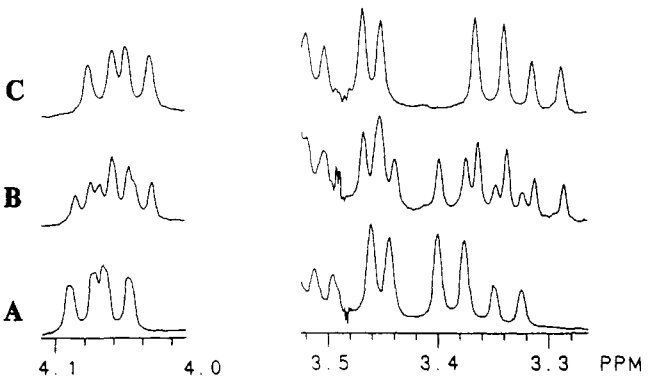

Figure 5. ^{1}H NMR spectra in the aliphatic region of bound tryptophan: (A) (*R*)-tryptophan + α-cyclodextrin; (B) (*RS*)-tryptophan + α-cyclodextrin; (C) (*S*)-tryptophan + α-cyclodextrin.

At this point we raise an important question. Are cyclodextrins inherently symmetrical and do they have C_n symmetry where n = number of glucose units in the oligomer? Based on our NMR results, the answer is yes. Based on computational studies, the answer is no. Using several different force fields, we find that symmetry breaking lowers the energy of these systems.[13] Hence, for α-CD, going from C_6 to C_3 to C_2 and lower symmetry decreases the energy of the macrocyclic host. The NMR results presented here, then, are time-averaged structures only.

2. Guest–Host Complexes. The macrocyclic cavity is best suited for complexation of substrate with small aromatic rings. Tyrosine, phenylalanine, and tryptophan are suitable substrates in this regard, and all three are sparingly soluble in water. Tyrosine has the lowest solubility. We were only able to make 1 mM tyrosine–αCD complexes. The enantiomers showed no differences in their NMR spectra at room temperature. When the enantiomers were cooled to 5 °C, the C_β protons started showing two sets of peaks but still were not well resolved. With phenylalanine we had similar problems although it displayed small separation at room temperture. Tryptophan was best suited for our studies, and the results are described here.

(*R*)-Tryptophan binds more tightly to α-CD than does the *S* antipode. Armstrong et al., using an α-CD chiral stationary phase, demonstrated the enantioselectivity of α-CD toward aromatic amino acids.[14] The separability factor α is related to the differential free energy of binding by $\Delta\Delta G = -RT \ln \alpha$. The observed value of $\alpha = 1.20$ corresponds to a differential free energy dif-

(11) (a) Chandrasekaran, R.; Ramachandran, G. N. *Int. J. Peptide Protein Res.*, **1970**, *2*, 223. (b) Bhat, T. N.; Sasisekharan, V.; Vijayana, M. *Ibid.* **1979**, *13*, 170. (c) Janin, J.; Wodak, S.; Levitt, M.; Maigret, B. *J. Mol. Biol.* **1978**, *125*, 357. (d) Dezube, D.; Dobson, C. M.; Teague, C. E. *J. Chem. Soc., Perkin Trans. 2* **1981**, 730. (e) Engh, R. A.; Chen, L. X.-Q.; Fleming, G. R. *Chem. Phys. Lett.* **1986**, *126*, 365.

(12) (a) Wood, D. J.; Hruska, F. E.; Saenger, W. *J. Am. Chem. Soc.* **1977**, *99*, 1735. (b) Casy, A. F.; Mercer, A. D. *Magn. Reson. Chem.* **1988**, *26*, 765–74. (c) Qi, H. Z.; Ma, K. V.; Diaz, L.; Grant, D. M.; Chang, C. *J. Org. Chem.* **1991**, *56*, 1537–42.

(13) Lipkowitz, K. B. *J. Org. Chem.* **1991**, *56*, 6357.

(14) Armstrong, D. W.; Yang, X.; Han, S. M.; Menges, R. A. *Anal. Chem.* **1987**, *59*, 2594.

Table I. Tabulation of Chemical Shifts (δ) and Coupling Constants (J)[a]

(a) Chemical Shifts

assgnt	free Trp [δ_F] (δ(F))	(R)-Trp + α-CD ($\delta(R)$)	(S)-Trp + α-CD ($\delta(S)$)	$\Delta\delta(R)$ (δ(F) − $\delta(R)$)	$\Delta\delta(S)$ (δ(F) − $\delta(S)$)	$\Delta\Delta\delta$ ($\delta(R)$ − $\delta(S)$)
H_1 (Ar_1, d)	2319.89	2330.22	2329.43	−10.33	−9.54	−0.79
H_4 (Ar, d)	2260.48	2275.81	2269.55	−15.33	−9.07	−6.26
H_6 (Ar, s)	2193.28	2196.81	2196.75	−3.53	−3.47	−0.06
H_3 (Ar, t)	2184.25	2183.94	2183.85	+0.31	+0.40	−0.09
H_2 (Ar, t)	2158.69	2165.29	2161.31	−6.60	−2.62	−3.98
H_α	1214.92	1221.19	1217.63	−6.98	−2.71	−4.27
	1045.37	1043.56	1046.16	+1.81	−0.79	+2.60
$H_{\beta 1}$						
$H_{\beta 2}$	989.03	1008.86	998.41	−19.83	−9.39	−10.44

(b) Coupling Constants

assgnt	free Trp (J(F))	(R)-Trp + α-CD ($J(R)$)	(S)-Trp + α-CD ($J(S)$)	$\Delta J(R)$ (J(F) − $J(R)$)	$\Delta J(S)$ (J(F) − $J(S)$)	$\Delta\Delta J$ ($J(R)$ − $J(S)$)
H_1 (Ar, d)	7.87	7.82	7.79	0.05	0.08	0.03
H_4 (Ar, d)	8.17	7.97	8.07	0.20	0.10	0.10
H_3 (Ar, t)	7.58	7.04	7.02	0.54	0.56	0.02
H_2 (Ar, t)	7.48	7.55	7.69	0.07	0.21	0.14
H_α	8.07	6.72	7.72	1.35	0.35	1.00
	4.84	5.10	5.01	0.26	0.17	0.09
	8.07	7.38	7.83	0.69	0.24	0.45
$H_{\beta 1}$	4.84	5.03	5.02	0.19	0.18	0.01
$H_{\beta 2}$	8.07	7.41	7.86	0.66	0.21	0.45
	4.84	4.98	4.91	0.14	0.07	0.07

[a] Chemical shifts are expressed in units of hertz and coupling constants (J) in units of hertz. $\Delta\delta(R)$ and $\Delta\delta(S)$ are the differences in free and bound states of (R)- and (S)-tryptophan with α-CD, respectively. $\Delta\Delta\delta$ is the difference in the bound states.

ference for substrate binding of ~400 cal mol^{-1}. This is a small difference that is expected to give subtle changes in the recorded spectra.

Figures 4 and 5 show ^{1}H NMR comparative spectra of the aromatic region and C_α and C_β proton regions, respectively. The center plot in each figure is the complex formed by racemic tryptophan with α-CD, and it is clearly evident that doubling of peaks exist. These peaks are simply the superposition of spectra from the individual diastereomeric inclusion complexes that have formed. The top and bottom traces are the enantiomerically pure (S)-tryptophan with α-CD and the (R)-tryptophan with the α-CD, respectively. The resulting changes in chemical shifts ($\Delta\delta$) and coupling constants (ΔJ) between free and bound tryptophan are tabulated in Table I.

It is well documented that inclusion complexes as described here are weak, and accordingly, the differences in free vs bound states of tryptophan are expected to be small. To better appreciate these small changes, we discuss them in frequency units (Hz) rather than the usual ppm units. This is allowed because we are comparing these values from a single spectrometer.

The assignments were made in Figure 3. Among the aromatic resonances the largest change in δ was observed on the H_4 doublet resonance. The difference between the R enantiomer in the bound state to the free state is given by ($\Delta\delta(R)$ = δ(free) − δ(R-bound)), which is equal to −15.33 Hz for this H_4 resonance. The same value for the S enantiomer in the bound state ($\Delta\delta(S)$) is equal to −9.07 Hz. The negative sign indicates a downfield shift when bound. Further, the difference between the two bound states is given by $\Delta\Delta\delta = \Delta\delta(R) - \Delta\delta(S)$, which is equal to −6.26 Hz for this H_4 resonance. Here again, the negative sign represents a larger downfield shift for the R enantiomeric complex. The H_1 doublet also had an appreciable downfield shift given by $\Delta\delta(R)$ = −10.33 Hz and $\Delta\delta(S)$ = −9.54 Hz. Because both R and S had almost equal shifts ($\Delta\Delta\delta$ = −0.79 Hz), this H_1 doublet could not be resolved in the central plot in Figure 4. The singlet resonance (H_6) has a small and equal downfield shift for both the R and S complex. Of the remaining two triplet resonances, one corresponding to H_3 has very little or no change at all and the other (H_2) triplet showed some small downfield shift given by $\Delta\delta(R)$ = −6.60 Hz, $\Delta\delta(S)$ = −2.62 Hz, and $\Delta\Delta\delta$ = −3.98 Hz. Moving to the C_α proton resonance, we find some differences as $\Delta\delta(R)$ = −6.98 Hz, $\Delta\delta(S)$ = −2.71 Hz, and $\Delta\Delta\delta$ = −4.27 Hz. Finally, among the C_β protons, C_β H_1 had small changes but it is the only place where the sign was different. That is, $\Delta\delta(R)$ = +1.81 Hz, representing an upfield shift, $\Delta\delta(S)$ = −0.79 Hz, representing a downfield shift, and $\Delta\Delta\delta$ = +2.6 Hz. The remaining C_β H_2 proton showed the highest changes of all resonances given by $\Delta\delta(R)$ = −19.83 Hz, $\Delta\delta(S)$ = −9.39 Hz, and $\Delta\Delta\delta$ = −10.44 Hz.

So, from chemical shift information, we see that the aromatic H_4 and C_β H_2 resonances show maximum changes. In all cases, the (R)-tryptophan + α-CD complex shows more downfield shift compared to the (S)-tryptophan + α-CD complex except in the case of C_β H_1 where there is a small upfield shift. It is known from earlier studies of inclusion complexes that aromatic rings prefer to be inside the cavity of CD which is hydrophobic. In the case of tryptophan, this makes it easy for the indole ring NH to form a H bond with the secondary hydroxyl groups which are located at the rim of the CD. Aromatic H_4 and H_1 protons are better exposed to the CD atoms and show larger changes whereas the H_2 and H_3 protons are simply buried inside the cavity having less interaction with the CD atoms and, thus, demonstrate less changes. The strength of the indole NH hydrogen bond with the acetal linker oxygens and with the secondary hydroxyl groups vary between the two complexes, and this leads to differences in $\Delta\Delta\delta$ (vide infra). In a similar way, the relatively larger changes observed in C_α and C_β proton resonances can be explained.

Similar changes in the ^{13}C NMR spectra were also observed. Figures S3 and S4 (supplementary material) show ^{13}C proton coupled and decoupled spectra of the aromatic region and of the C_α and C_β regions in free and bound states, respectively. Here again, we observe doubling of many of the aromatic resonances and of the C_α carbon whereas the C_β carbon did not show any changes.

Although modest changes in differential chemical shifts were observed for R vs S guest, very few changes in coupling constants were found. The largest difference listed in Table I is around 1 Hz for the C_α proton. The results from Table I indicate that small changes in conformation occur upon complexation but that those changes are about the same for (R)- and (S)-tryptophan.

To further explore differences in these weakly bound diastereomeric complexes, T_1 measurements were made on free tryptophan, free α-CD, and the individual R and S complexes. The results are presented in Table II. It is seen in the table that there is a substantial reduction in T_1 values for tryptophan protons when complexed with α-CD. Here we have an interesting situation. As seen in the table, free tryptophan has relatively high T_1 values.

Table II. Tabulation of T_1 Values (s) for Tryptophan Resonances and α-CD Resonances[a]

(a) Tryptophan Resonances

assgnt	free Trp (T_{1F})	(*R*)-Trp + α-CD (T_{1R})	(*S*)-Trp + α-CD (T_{1S})	ΔT_{1_R} ($T_{1R} - T_{1F}$)	ΔT_{1_S} ($T_{1S} - T_{1F}$)	$\Delta\Delta T_1$ ($\Delta T_{1R} - \Delta T_{1S}$)
H_1 (Ar, d)	1.60	0.98	0.98	−0.62	−0.62	0.00
H_4 (Ar, d)	3.10	1.14	1.58	−1.96	−1.52	−0.44
H_6 (Ar, s)	3.85	3.65	3.65	−0.20	−0.20	0.00
H_3 (Ar, t)	1.72	0.98	0.98	−0.74	−0.74	0.00
H_2 (Ar, t)	1.50	0.70	0.86	−0.80	−0.64	−0.16
H_α	1.70	0.97	1.19	−0.73	−0.51	−0.22
$H_{\beta 1}$	0.44	0.17	0.26	−0.27	−0.18	−0.09
$H_{\beta 2}$	0.49	0.20	0.27	−0.29	−0.22	−0.07

(b) α-CD Resonances

assgnt (on α-CD)	free α-CD T_{1F}	α-CD + Trp (T_{1B})	ΔT_1 ($T_{1B} - T_{1F}$)	assgnt (on α-CD)	free α-CD T_{1F}	α-CD + Trp (T_{1B})	ΔT_1 ($T_{1B} - T_{1F}$)
H_1	0.40	0.48	+0.08	H_5	0.26	0.31	+0.05
H_3	0.67	0.60	−0.07	H_2	0.069	0.80	+0.11
H_6	0.20	0.27	+0.07	H_4	0.37	0.44	+0.07

[a] (−) indicates decrease and (+) indicates increase in T_1 values.

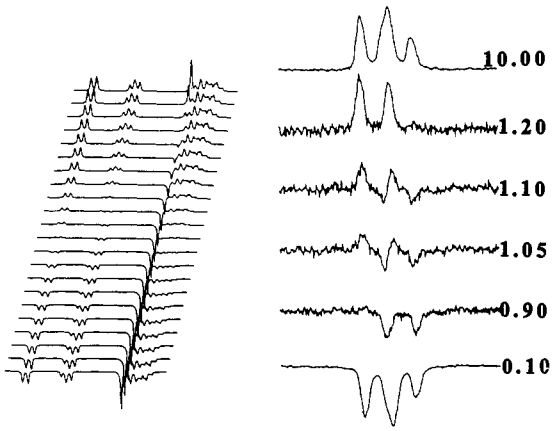

Figure 6. Left: Stack plot of aromatic region T_1 plots of (*RS*)-tryptophan + α-cyclodextrin. Right: Blow up of T_1 plots with close τ values. Top and bottom traces are from the highest and lowest τ values. Individual τ values in seconds are indicated on the corresponding spectrum.

Free α-CD has the smallest T_1 values. T_1 of tryptophan reduces on complexation but, interestingly, is higher than the α-CD T_1 values. These results are indicative of weak coupling between tryptophan and α-CD, which, from a dynamical aspect, has been previously shown for aromatic compounds with cyclodextrins.[15] This means the guest and host molecules can perform different molecular motions. The correlation times τ_c of the guest molecules are 4–6 times shorter than those of α-CD. Thus, tryptophan, though complexed, still has a faster τ_c, and this is the reason it still maintains a relatively higher T_1.

The relationship between T_1 and $\omega\tau_c$ is well-known.[16] T_1 goes through a minimum when $\omega\tau_c \approx 1$. In liquids, for small organic molecules, τ_c is typically 10^{-11}–10^{-10} s, and for large systems like biomolecules it is around 10^{-8}–10^{-7} s. Cyclodextrins with molecular weights near 1000 straddle these two extremes. In this light it is to be noted that the α-CD has a low T_1 value in its free state but shows a very slight increase upon complexation. This is because of a slight increase in the overall τ_c (presumably because of less hydrogen bonding to the solvent) which shows up as an increase in T_1. The only exception is the H_3 nucleus of α-CD which, on the contrary, displays a slight decrease in its T_1 value upon complexation. This is because it has an additional pathway through interaction with the H_4 proton of the included tryptophan (see NOE results below).

This effect is more pronounced when we look in the reverse direction, that is, by considering H_4 of tryptophan. The T_1 change on tryptophan H_4 displays the largest difference upon binding. For (*R*)-tryptophan in the free state T_1 = 3.10 s and, upon complexation, is reduced to 1.14 s. For the *S* antipode this reduces to only 1.58 s. This difference in reduction is attributed to tighter binding of (*R*)-tryptophan. Pictorially, these T_1 changes are shown in Figure 6 where on the right side the tryptophan H_4 proton is blown up. This part of the figure has plots with close delay times for the inversion-recovery experiments.

The sample is racemic tryptophan plus α-CD. Because of differential binding we find two doublets that, due to overlap, appear as a triplet. In the lower trace both doublets have negative intensity. As one ascends the traces, τ increases and a nice separation is observed. At one point both doublets are clearly separated, one having a positive intensity and the other negative intensity. This differential change in relaxation rates of H_4 in the complex is a direct consequence of (*R*)-tryptophan binding more tightly than (*S*)-tryptophan.

As mentioned above, the sizes of the inclusion complexes studied here fall in the region where $\omega\tau_c \approx 1$, and our complexes lie in the region where NOE is close to zero. Nonetheless, we did attempt to look for NOE enhancements and we did succeed in locating an important intermolecular NOE, apart from some intramolecular NOEs. The intramolecular NOEs of tryptophan were discussed earlier. Upon complexation, the same NOEs exist but there is a reduction in the percent enhancement as expected. The relative percent enhancements are compiled in Table III. Again, consistent with tighter binding, the *R* enantiomer shows a relatively larger reduction. One may presume, based on the

Table III. Tabulation of Intramolecular NOE Enhancement Percentages

irradiation at	NOE seen at	on free Trp	on (*R*)-Trp + α-CD complex	on (*S*)-Trp + α-CD complex
H_1	H_2	13.3	1.5	5
H_1	H_α	7	1.3	1.5

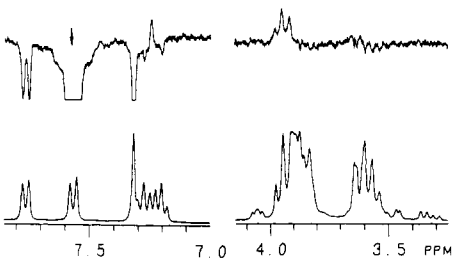

Figure 7. Intermolecular NOE enhancement of the tryptophan + α-cyclodextrin complex. Arrow indicates irradiation of tryptophan H_4 proton. An NOE of 0.5% is observed on the α-cyclodextrin H_3 proton.

(15) Behr, J. P.; Lehn, J.-M. *J. Am. Chem. Soc.* **1976**, *98*, 1743.
(16) Akitt, J. W. *NMR and Chemistry—An Introduction to the Fourier Transform Multinuclear Era*; Chapman and Hall: New York, 1983.

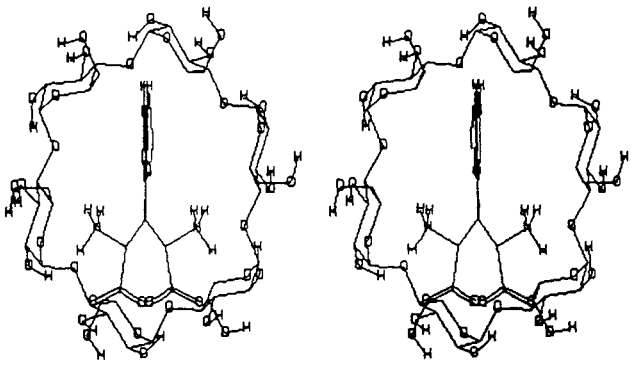

Figure 8. Stereoview of tryptophan embedded in α-cyclodextrin. The *R* and *S* guests have been superimposed to show they both start along a 6-fold symmetry axis. View is from the primary hydroxyl side of the host, and hydrogens have been removed for clarity.

preceding discussion of T_1 changes, that the reduction of intramolecular NOEs in the bound state relative to the free state is attributed to the slowing of the molecular motion of the amino acid. An alternative explanation is that a change in conformation of the tryptophan, induced by complexation, has taken place. This latter explanation is not consistent with the results of the molecular dynamics simulations described later. Figure 7 shows the intermolecular NOE difference spectra of the complex. The irradiation is on the tryptophan H_4 which results in only 0.4% enhancement on H_3 of α-CD. No other intermolecular NOEs could be detected. These results show that these protons are in close proximity and they are fully consistent with the corresponding relaxation rates (T_1 data) discussed above. The most intriguing point derived from our study of intermolecular NOEs is that both (*R*)-tryptophan and (*S*)-tryptophan have the same magnitude NOE to the same proton on α-CD. This suggests that the complex formation is similar in both cases. All of this is consistent with the simulation results described below.

B. Molecular Modeling and Dynamics Simulation. The main problem encountered in this study is that we are attempting to compute exceedingly small free energy differences (<kT). However, as we pointed out earlier, if one samples configurations for statistical averaging such that the *R* and *S* enantiomers are treated the same way, one can reliably compute these small differences.[17] There are two points to consider in this regard. The first involves the inherent reliability of the force field itself. Generally, when one considers computed bond lengths, bond angles, conformational energies, etc., the experimental vs theoretical results are better for a related set of molecules than when comparing unrelated systems. For our studies, we are comparing enantiomers. They have the same shapes, same electrical features, and so on. Any deficiencies in the force field, then, will be exactly the same for both enantiomers and nearly the same for both diastereomeric complexes. The second point involves sampling the microstates. To ensure no artifacts are included in the calculation, e.g., sampling a low-energy region for one complex but sampling a high-energy region for the other, we treat both systems the same way. Hence, deficiencies in the force field tend to cancel because we are comparing nearly identical molecular assemblies, and artifacts from sampling configurations which are used for statistical averaging are minimized. The net result is a cancellation of errors that allow us to compute relatively small energy differences with confidence.[6]

1. Docking Orientations. The minimum energy conformation of tryptophan that is consistent with NMR results (H_4 near H_α) was used for binding to α-CD. Although C_6 symmetric α-CD is of higher energy than the less symmetric conformers, we use it to initially dock the substrates and then we allow the macrocycle to mold itself around the guest by energy minimization. The plane of tryptophan's aromatic ring is aligned along one of the symmetry planes of C_6 α-CD. The ring is embedded just deep enough into the secondary hydroxyl rim of the cavity so the ammonium and carboxylate groups come into contact with the secondary OH groups. A stereoview representing this first maneuver in our docking strategy is shown in Figure 8.

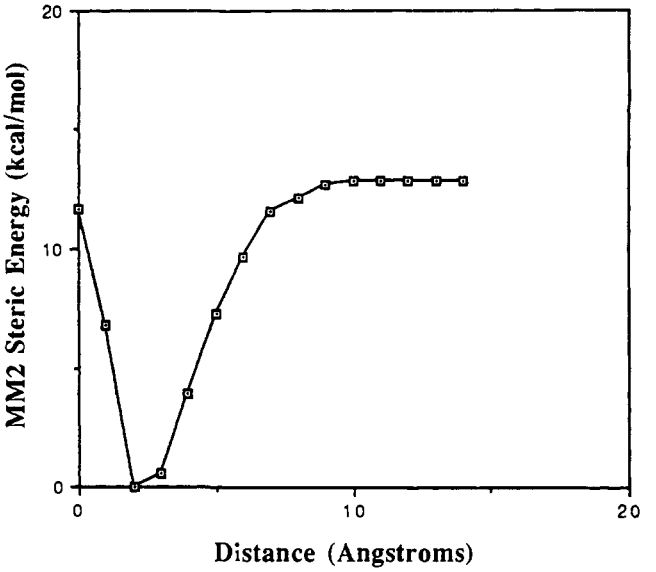

Figure 9. MM2 steric energy of benzene as it is constrained to move into the interior of α-cyclodextrin. The abscissa corresponds to the distance between benzene's nearest hydrogen and the macrocycle's center of mass (see text for details).

The view is looking up from the primary OH rim toward the secondary OH rim, and the *R* enantiomer has the ammonium and carboxylate pointed toward the right while *S* has them pointed left. Each diastereomer, starting from these positions, is, in turn, energy minimized followed by the MD simulation.

How deeply embedded into the cyclodextrin is the aromatic ring? We find it not to be deeply sequestered within the cavity at all. Indeed, we find it further out of the cavity than we expected, not because the tryptophan's pendant groups prevent it from slipping in, but rather, because the equatorial belt of acetal linker oxygen's holding the macrocycle together make the interior of the host very constricted. Figure 9 shows the steric energy of a complex formed from benzene with α-CD as a function of benzene's distance from the interior of the cavity. These results were evaluated with MM2 as implemented in MACROMODEL[18] the following way.

An origin and three orthogonal axes are placed at the center of mass of a C_6 α-CD. This places the origin nearly in the plane of the six acetal linker oxygens with the *z* axis aligned with the C_6 symmetry axis of the CD. Hydrogen atoms 1 and 4 of benzene are held fixed along this axis, and the marked (*) hydrogen is set at the origin. The 1,4-hydrogens of benzene are allowed to move in the *x* and *y* directions but not *z*. Atoms O_5 in monomers A and D (see Figure 1) are likewise constrained in the *z* direction. This is to prevent the CD from "following" the benzene molecule as it is moved up and down the *z* axis. The remainder of the CD and benzene is allowed to fully relax. Beginning with the asterisk-labeled H at $z = 0.0$, the system is geometry optimized using a block-diagonal Newton Raphson minimizer. The C_6 symmetry of α-CD is lost, and a C_2 symmetric complex results. The benzene is then incrementally pulled out of the cavity in 1-Å increments along the *z* axis beginning from the previously minimized structure to produce the reaction coordinate displayed in Figure 9. The key feature of this plot is that the asterisk-labeled H of benzene is fully 2 Å from the middle of the macrocycle cavity at its minimum energy and the middle of the benzene ring is even further removed. The bottleneck for moving benzene through a C_2 α-CD is larger than anticipated.

(17) Lipkowitz, K. B.; Baker, B.; Zegarra, R. *J. Comput. Chem.* **1989**, *10*, (5), 718.

(18) Mohamadi, F.; Richards, N. G. J.; Guida, W. C.; Liskamp, R.; Lipton, M.; Caufield, C.; Chang, G.; Hendrickson, T.; Still, W. C. *J. Comput. Chem.* **1990**, *11*, 440.

Table IV. Averaged Energies[a] of (R)- and (S)-Tryptophan with α-CD Face-Down (kcal mol^{-1})

	R (100 ps)	S (100 ps)
total potential energy	132.96	137.74
bond	33.42	35.21
angle	118.05	117.95
torsion	29.07	28.15
improper	3.65	5.39
total internal energy	184.21	186.71
VDW	-5.19	-4.62
Coulomb	-44.06	-44.35
total external energy	-49.24	-48.97

[a] Configurational sampling done every 10 fs for statistical averaging.

Table V. Averaged Energies[a] of (R)- and (S)-Tryptophan with α-CD Face-Up (kcal mol^{-1})

	R (100 ps)	S (100 ps)
total potential energy	132.77	137.37
bond	34.74	34.95
angle	118.77	118.69
torsion	28.54	30.73
improper	4.11	3.97
total internal energy	186.17	188.35
VDW	-7.48	-6.00
Coulomb	-45.92	-45.97
total external energy	-53.40	-51.97

[a] Configurational sampling done every 10 fs for statistical averaging.

2. Differential Binding Energies. The aforementioned gas-phase binding enthalpies are intended to show where a benzene tends to reside as it is constrained to slide up and down a C_2 symmetry axis of cyclodextrin. Without the constraints imposed above, the benzene tends to become orthogonal to the z axis and pack into the macrocycle near the secondary OH rim. This mode of aromatic ring binding is also evident in the binding of tryptophan. Upon energy minimization of the 6-fold symmetric α-CD with tryptophan embedded in it, the R enantiomer slides off toward the right and the S enantiomer to the left while the indole ring resides near the cavity opening (but not out of it). This places the tryptophan H_4 in proximity to the α-CD H_3. This was confirmed by our NMR results.

There are actually two ways the indole can tilt from the C_6 axis, and both were examined. One way has the stereogenic center pointed away from the interior of the α-CD while the CO_2^- and NH_3^+ retain contact with secondary OH groups, and the other way has the stereogenic center pointed toward the interior of the macrocyclic ring. The former orientation is heretofore called "up"

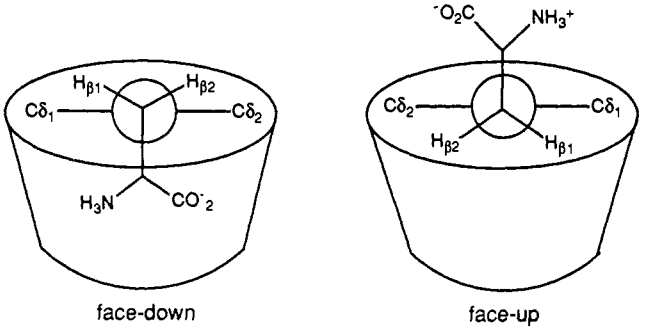

and the latter is "down". Again, irrespective of orientation of substrate with respect to receptor, whatever was done to the R guest was done to the S guest.

These initial starting conditions allowed us to carry out successful MD simulations, the results of which are presented in Tables IV and V. Consistent with experiment, the R enantiomer is more tightly bound than its optical antipode, and, as anticipated, the computed differential binding energies are overestimated. They are overestimated because no explicit inclusion of solvent was taken into consideration and a very low dielectric constant of 1.5 was used in the simulation. Of the two orientations, the one with the stereogenic center face up is consistently lower in energy for both R and S guests than when they are face down.

Table VI. Distribution of Hydrogen Bonds Formed in (R)- and (S)-Tryptophan Complexes

no. of intermolecular H bonds	no. of configns S	no. of configns R	no. of intermolecular H bonds	no. of configns S	no. of configns R
0	47	5	3	30	397
1	639	81	4	5	163
2	279	344	5	0	10

Included in the tables are the energy components that sum up to the total potential energy. These energies depend on the potential functions and their associated parameters that make up the force field and, accordingly, are force field dependent. They have little physical significance. Nonetheless, we provide these energies to examine how the individual terms comprising this particular force field differ in the R vs S complexes. In Table V the largest differences in energy appear in the torsion and van der Waals terms. The R enantiomer is thus more tightly bound in part because the system has less torsional strain and because the nonbonded interactions are more favorable. Table IV shows the largest differences arise from changes in bond lengths and improper dihedral angles. Both tables indicate similar electrostatic interactions for R and S substrate regardless of their orientation.

These component energies are also partitioned into internal and external energies. The internal energy is simply the sum of the first four component energies, and the external energy is the sum of the van der Waals and electrostatic contributions. Both tables indicate the external energy to favor the R enantiomer and the internal energy to favor the R enantiomer when averaged over the duration of the simulation.

3. Chiral Recognition. It would be easy to say at this point that, based on the results of Table V, the origins of enantioselection arise from less torsional strain along with more favorable nonbonded contacts for the R enantiomer. But, we would like to develop a more defined chiral recognition model, and we begin by examining the hydrogen-bonding patterns in the two complexes. First, we examine the number of times each of 1000 uniformly sampled structures from the simulation can form a hydrogen bond, and then we consider where the hydrogen bonds between guest and host appear.

As tryptophan diffuses through solution, either in a chromatographic flow or in a spinning NMR tube, it encounters and binds with the cyclodextrin to form a short-lived diastereomeric complex. Not all encounters lead to productive binding, and not all binding is expected to be in the most stable orientation. In our simulations we consider only binding to the interior of the macrocycle because of literature precedence for inclusion complexation[3] and because of our NMR studies described above. Of the two simulations carried out, both indicate the (R)-tryptophan is more tightly bound. However, the face-up orientation is approximately 2 kcal mol^{-1} more stable than the face-down orientation. The face-up orientation is, then, the more probable mode of binding. It is certainly possible that other orientations and modes of guest–host complexation exist, but we did not pursue these because our simulations are consonant with NMR and chromatography data. Therefore, we restrict our discussion to the face-up orientation only.

For our purposes a hydrogen bond of the type H···A–X exists when the distance between H and A is ≤2.5 Å, the distance between H and X is ≤3.3 Å, and the HAX angle ≥90°. The type of hydrogen bonds (single, double, ..., multiple) and the number of them formed between tryptophan and α-CD are listed in Table VI. Of 1000 uniformly sampled configurations, there were 47 that had no intermolecular hydrogen bonds for (S)-tryptophan and five with no hydrogen bonds for (R)-tryptophan. There were 639 configurations with a single intermolecular hydrogen bond for S and 81 for R. It is to be noted that the distributions reported in Table VI are significantly different. Here one observes a substantially larger number of simultaneous multiple-contact

Table VII. Allocation of H Bonds between Tryptophan and α-Cyclodextrin

	(*R*)-tryptophan				(*S*)-tryptophan			
	O_{25}	O_{26}	NH	NH_3	O_{25}	O_{26}	NH	NH_3
CD Groups								
C_2 hydroxyl	240	362	92	0	426	501	0	2
C_3 hydroxyl	791	776	0	11	16	72	162	0
O_1	0	0	930	0	0	0	128	0
total	1031	1138	482	11	442	573	290	2

hydrogen bonds for *R* than for *S*. Thus, there are two key findings. First, the *R* enantiomer forms a greater number of intermolecular hydrogen bonds (2668 *R* vs 1307 *S*; this will be discussed later), and *R* forms a larger number of multiple-contact hydrogen bonds than does *S*.

A somewhat more detailed assessment of the hydrogen-bonding patterns that form in the two complexes is presented in Table VII. Here we see how the hydrogen bonds are allocated. The sum total of the hydrogen bonds in the *R* complex is 2662 and for *S* is 1307 as stated above. Fully 81% of the intermolecular hydrogen bond contacts are made by the two carboxylate oxygens for the *R* enantiomer, and the rest come mainly from the indole N–H. For the *S* enantiomer, 78% of the hydrogen bond contacts arise from the carboxylate and the remainder from the N–H. The big difference between *R* and *S* guests, then, is the number of hydrogen bonds that form rather than the way these hydrogen bonds are allocated. Furthermore, it is noted in Table VII that the indole N–H can form a substantial number of hydrogen bonds to the equatorial belt of acetal linker oxygens. The *R* enantiomer forms relatively more of these than *S*, suggesting slightly different time-averaged tilts of the aryl ring of the guest or, perhaps, that the *R* substrate is more deeply sequestered in the host's cavity.

The number and location of all the hydrogen bonds formed over the duration of the simulation are depicted graphically in Figure 10. The large circle represents the host cavity, and the black dots on that circle represent the acetal oxygens linking together the glucose monomers (O_1 in Figure 1). The lines pointing in a clockwise orientation represent the secondary hydroxyl O–H bond vectors on the rim of the cavity. The C_2 hydroxyl and C_3 hydroxyl groups are secondary alcohols that can serve as hydrogen bond donors (D) as well as hydrogen bond acceptors (A). The groups on the tryptophan capable of hydrogen bonding are the two carboxylate oxygens (A), the indole N–H (D), and the ammonium group (D). The number of times a hydrogen bond occurs at a given site on the CD is represented by the filled circles whose radii increase with the number of H bonds formed at that particular site. The cross-hatchings are codes to indicate which group on the tryptophan is participating.

Three features emerge. The first feature to emerge is that both complexes are highly localized and the *R* guest binds to one side of the macrocycle while *S* binds to the other. One may argue that these simulations are too short to be realistic and the hydrogen-bonding patterns arise simply from our initial conditions. However, similar plots for the face-down orientation indicate far less localization, with the tryptophan freely roaming around the interior of the cavity during a simulation of identical time period. Indeed, a comparison of the face-down with face-up simulation indicates that if the less stable face-down orientation forms, it slides around the interior of the CD cavity looking for suitable hydrogen-bonding sites and then leaves the cavity or flips to the more stable face-up orientation where it becomes more tightly coordinated.

The second feature to emerge involves the number of hydrogen bonds. The *R* enantiomer forms nearly twice as many hydrogen bonds as *S*. Our rationale for this is that the carboxylate oxygens of the (*R*)-tryptophan can readily accept a hydrogen bond from the macrocycle and the tryptophan can readily donate a hydrogen bond, via the indole N–H, to the secondary hydroxyls on the macrocycle. The carboxylate oxygens of the *S* enantiomer can also accept hydrogen bonds, but the indole N–H finds it difficult to donate to the secondary hydroxyls on the host. The reason for this is that the N–H of the *S* enantiomer must first push itself through the hydrogen atoms of the hydroxyl groups before it can attach to the hydroxyl's oxygen on the host. For the *R* enantiomer the directionality of the secondary OH bond vectors is such that the oxygens are more accessible. The *S* enantiomer's N–H is thus in a less hospitable environment for hydrogen bond donation to the rim of the α-CD than is the N–H of the *R* enantiomer.

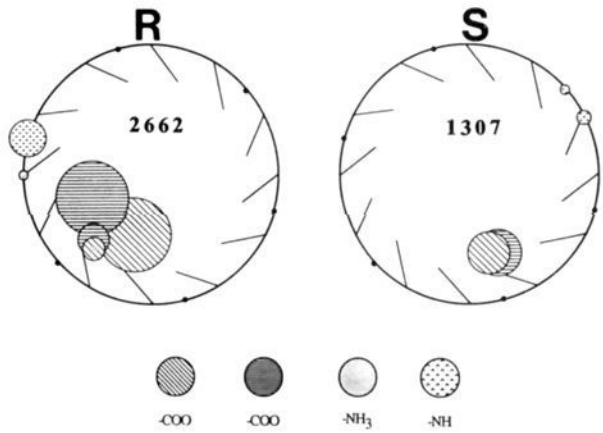

Figure 10. Graphical representation of the intermolecular hydrogen bonds of (*R*)- and (*S*)-tryptophan with α-cyclodextrin. The large circle represents the macrocyclic host. The small black dots on that circle are the acetal linker oxygens, and the lines attached to the circle represent the unidirectional C_2 and C_3 hydroxyl groups. The cross-hatching indicates the atoms or groups of atoms on the tryptophan that are forming the intermolecular hydrogen bonds. The size of the cross-hatched circle corresponds to the number of hydrogen bonds formed during the simulation. The centers of the cross-hatched circles are placed at the mean positions of the hydrogen bond contacts.

The third feature to emerge is that hydrogen bonding occurs primarily from the tryptophan's carboxylate and indole N–H groups irrespective of the chirality of the guest. The ammonium group in both cases projects up and out of the interior of the host. Based on this, then, we predict that replacing the NH_3^+ with $N(Me)_3^+$ will have little or no effect on the chiral recognition. This, in turn, means the chromatographic separability factors α will be nearly the same as in tryptophan itself but that larger capacity factors *k* are expected due to enhanced hydrophobic binding of guest to host.

Finally, we take note that the number of hydrogen bonds formed is not an indication of overall hydrogen bond strength. One may find cases where a smaller number of strong hydrogen bonds in one complex is more stabilizing than a large number of weak hydrogen bonds in another complex. To address this, we computed the hydrogen bond component energy of the total force field energy averaged over the simulation. The average intermolecular hydrogen bond energy in the *R* complex is −5.84 kcal mol^{-1} and that in the *S* complex is −2.80 kcal mol^{-1}.

Summary

In this paper we examined the enantioselective binding of tryptophan to α-cyclodextrin. Free and bound tryptophan were examined by NMR spectroscopy. Most resonances of tryptophan experience deshielding upon coordination. Differential chemical shifts $\Delta\Delta\delta$ between *R* and *S* guests consistently show larger shifts for the *R* enantiomer which is fully consistent with chromatographic retention orders and theory described in this paper. T_1 of tryptophan reduces on complexation but is still higher than T_1 of cyclodextrin, indicating weak coupling between the dynamical

motions of guest and host. The changes in T_1 times as guest binds to host for the *R* enantiomer are larger than for *S*, again indicative of tighter *R* binding. The changes in inter- and intramolecular NOEs were also measured. Upon complexation, the same NOEs exist as in the free state but there is a reduction in the percent enhancement, again with the *R* tryptophan having the larger changes. An intermolecular NOE between tryptophan and cyclodextrin reveals the tryptophan aromatic H_4 to be near the cyclodextrin's H_3. The H_3 proton is on the interior of the macrocycle pointing in toward the cavity. A small NOE of similar magnitude for *R* and *S* enantiomers was found.

Gas-phase molecular simulations reveals that (*R*)-tryptophan forms a larger number of hydrogen bonds than does (*S*)-tryptophan, but more interestingly, it forms a larger number of multiple-contact hydrogen bonds. The number and location of intermolecular hydrogen bonds reveal three features. First, both complexes are highly localized in spite of weak intermolecular association. Second, the (*R*)-tryptophan forms twice as many hydrogen bonds as (*S*)-tryptophan, and the average intermolecular hydrogen bond energy for *R* is almost 3 kcal mol^{-1} more than for *S*. Third, the intermolecular hydrogen bonds arise from the tryptophan carboxylate oxygens and its indole N-H rather than from the ammonium group.

A previously proposed chiral recognition model is consistent with our results. Armstrong advocates four requirements for chiral recognition:[19] (a) an inclusion complex must form, (b) a tight fit of the included species with the host cavity must exist, (c) the stereogenic center should be able to form one strong interaction with the hydroxyl groups of the CD cavity entrance, and (d) the unidirectional 2- or 3-hydroxyl groups at the secondary face of the macrocycle are especially important for chiral recognition. Based on our experimental work, we find inclusion complexation but with the aromatic ring of the guest tilted and near the top of the cavity rather than deeply embedded in it along a C_6 symmetry axis. Point b is hard to measure, but we find the tryptophan molecules to be highly localized on the interior of the cavity effectively behaving like a tight fit. We propose, then, to modify this criterion to be a tight fit or a high localization of guest with host. The third requirement is met by the carboxylate, and the last point, interaction with the unidirectional 2- or 3-hydroxyl groups, has been fulfilled. This latter criterion appears to be the key element of differentiation although we recognize the CD as a whole to be chiral. The directionality of the secondary hydroxyl OH bond vectors is such that the indole N-H finds the host's secondary OH oxygens accessible for hydrogen bonding. The indole N-H of the *S* guest, in contrast, is impeded by the hydrogen atoms of those hydroxyl groups. This results in fewer hydrogen bonds, less multiple-contact hydrogen bonds, and less stabilization of the complex.

Acknowledgment. This work was funded by the donors of the Petroleum Research Fund, administered by the American Chemical Society, and by a grant from the National Science Foundation (CHE-8901828).

Registry No. D-Trp, 153-94-6; L-Trp, 73-22-3; DL-Trp, 54-12-6; α-CD, 10016-20-3.

Supplementary Material Available: Tables of chemical shifts and coupling constants for α-CD, ^{1}H and ^{13}C NMR spectra of α-CD, and ^{13}C proton-decoupled spectra of the aromatic and C_α, C_β regions (4 pages). Ordering information is given on any current masthead page.

(19) (a) Ward, T. J.; Armstrong, J. *Liq. Chromatogr.* **1986**, *9* (2 & 3), 407. (b) Armstrong, D. W.; Ward, T. J.; Armstrong, R. D.; Beesley, T. E. *Science (Washington, D.C.)* **1986**, *232*, 1132.

exo,exo-[1,3-Bis(trimethylsilyl)allyl]lithium–*N,N,N',N'*-Tetramethylethylenediamine Complex: Crystal Structure and Dynamics in Solution

Gernot Boche,*,† Gideon Fraenkel,‡ José Cabral,‡ Klaus Harms,† Nicolaas J. R. van Eikema Hommes,§ John Lohrenz,† Michael Marsch,† and Paul von Ragué Schleyer*,§

Contribution from the Fachbereich Chemie, Universität Marburg, Hans-Meerwein-Strasse, D-3550 Marburg, Federal Rupublic of Germany, Department of Chemistry, The Ohio State University, Columbus, Ohio 43210, and Institut für Organische Chemie, Friedrich-Alexander-Universität Erlangen-Nürnberg, Henkestrasse 42, D-8520 Erlangen, Federal Republic of Germany. *Received July 19, 1991*

Abstract: The X-ray structure of the title compound (**1**·TMEDA) shows that the essentially symmetrical allyl anion moiety is perturbed by complexation with TMEDA in a twisted conformation. The NMR-observed symmetrization of both the allyl end carbons and all the TMEDA methyl groups at higher temperatures is best modeled by molecular orbital calculations when two mechanisms (ligand rotation and ligand twisting) are assumed. These are calculated to have nearly the same barrier and are in accord with the experimental value.

Introduction

Fraenkel, Chow, and Winchester recently[1] showed via ^{13}C and ^{1}H NMR, as well as a Saunders deuterium perturbation experiment,[2] that the *exo,exo*-[1,3-bis(trimethylsilyl)allyl]lithium–*N,N,N',N'*-tetramethylethylenediamine complex (**1**·TMEDA) in diethyl-d_{10} ether was "electronically symmetrical and exists in the exo configuration". The small ^{13}C NMR shift difference (0.48 ppm) between C(1) and C(3) of allyl in **1**·TMEDA and the large

† Universität Marburg.
‡ The Ohio State University.
§ Universität Erlangen-Nürnberg.

(1) Fraenkel, G.; Chow, A.; Winchester, W. R. *J. Am. Chem. Soc.* **1990**, *112*, 1382.
(2) (a) Saunders, M.; Telkowski, L.; Kates, M. R. *J. Am. Chem. Soc.* **1977**, *99*, 8070. (b) Faller, J. H.; Murray, H. H.; Saunders, M. *Ibid.* **1980**, *102*, 2306.

0002-7863/92/1514-1562$03.00/0